Communication: Three-dimensional model for phonon confinement in small particles: Quantitative bandshape analysis of size-dependent Raman spectra of nanodiamonds

Vitaly I. Korepanov, Henryk Witek, Hajime Okajima, Eiji sawa, and Hiro-o Hamaguchi

Articles you may be interested in

Probing confined acoustic phonons in free standing small gold nanoparticles
J. Appl. Phys. **113**, 074303 (2013); 10.1063/1.4792654

Effect of particle size and annealing on spin and phonon behavior in TbMnO3
J. Appl. Phys. **109**, 064309 (2011); 10.1063/1.3563571

Size-dependent magnetic properties and Raman spectra of La 2 NiMnO 6 nanoparticles
J. Appl. Phys. **106**, 123901 (2009); 10.1063/1.3269707

ZnO nanoparticle size-dependent excitation of surface Raman signal from adsorbed molecules: Observation of a charge-transfer resonance
Appl. Phys. Lett. **91**, 221106 (2007); 10.1063/1.2817529

Improved one-phonon confinement model for an accurate size determination of silicon nanocrystals
J. Appl. Phys. **86**, 1921 (1999); 10.1063/1.370988

Re-register for Table of Content Alerts

Create a profile.   Sign up today!

Communication: Three-dimensional model for phonon confinement in small particles: Quantitative bandshape analysis of size-dependent Raman spectra of nanodiamonds

Vitaly I. Korepanov,[1] Henryk Witek,[1] Hajime Okajima,[1] Eiji Ōsawa,[2] and Hiro-o Hamaguchi[1,a)]

[1]*Department of Applied Chemistry, National Chiao Tung University, 1001 University Road, Hsinchu, Taiwan 30010*

[2]*Nano-Carbon Research Institute, Ltd., 3-15-1 Tokida, Ueda, Nagano 386-8567, Japan*

Raman spectroscopy of nano-scale materials is facing a challenge of developing a physically sound quantitative approach for the phonon confinement effect, which profoundly affects the phonon Raman band shapes of small particles. We have developed a new approach based on 3-dimensional phonon dispersion functions. It analyzes the Raman band shapes quantitatively in terms of the particle size distributions. To test the model, we have successfully obtained good fits of the observed phonon Raman spectra of diamond nanoparticles in the size range from 1 to 100 nm. © 2014 AIP Publishing LLC. [http://dx.doi.org/10.1063/1.4864120]

Small particles show unique behaviors due to their spatial constraints. The phonon confinement effect is one of these unique physical characteristics of small particles. Because of limited coherence lengths, phonons of small particles are confined and behave differently from those in infinite lattices. The confinement effect is formulated by multiplying a phonon wave function by a confinement function (for example, Gaussian), the width of which is determined by the particle size. The "confined" wave function is not anymore an eigenfunction of the wave vector q, but rather a superposition of eigenfunctions with different q. An important outcome of the phonon confinement effect is the breakdown of optical selection rules. With decreasing particle size, phonons with non-zero q-vector have increasing contributions to optical spectra, contrary to the fact that only phonons from the Brillouin zone (BZ) center ($q_0 = 0$) are allowed for infinite lattices. Conversely, analysis of size-dependent optical spectra will lead to deeper understanding of the phonon confinement effect in small particles, with highly useful information on the sizes and size distributions of those particles. It will provide a firm basis for size characterization, which is becoming a big issue in material science/technology with regard to the size-function relationship in small particles.

It is known that the Raman spectral patterns of nanoscale systems are sensitive to their size,[1] and the size dependence comes from the phonon confinement effect. The physical model for this size dependence was first suggested by Richter *et al.*[2] more than 30 years ago. The contribution of phonons with non-zero wave vector to the Raman spectrum is defined through the Fourier coefficients of the integral over q:

$$I(\omega) \cong \int \frac{|C(q_0, q)|^2}{(\omega - \omega(q))^2 + (\Gamma_0/2)^2} d^3q, \qquad (1)$$

where ω is wavenumber, q is wave vector, $C(q_0, q)$ is the Fourier coefficient mentioned above, $\omega(q)$ is the three-dimensional (3D) phonon dispersion function, Γ_0 is the natural bandwidth.

In principle, the calculation of this integral requires 3D integration. Typical approach, however, is to substitute the 3D phonon dispersion function $\omega(q)$ with some effective 1D curve, often derived from approximately averaged neutron diffraction data.[3] This leads to 1D integral

$$I(\omega) \cong \int_0^1 \frac{\exp(-q^2\sigma^2/4)^*4\pi q^2}{(\omega - \omega(q))^2 + (\Gamma_0(\sigma)/2)^2} dq. \qquad (2)$$

Here, the Fourier coefficients, derived from the Gaussian confinement function, take the form $|C(q_0, q)|^2 = \exp(-q^2\sigma^2/4)$, where σ is the particle size. This 1D approach is not applicable if the material shows a strong anisotropy of phonon dispersion. Well known example having such anisotropy is diamond, in which over-bending of the longitudinal phonon branch has been observed even for low wave vector:[4] while two of the optical phonon branches have a "downward" curvature near the BZ center, the third one has an "upward" curvature. Obviously, effective 1D function cannot represent well for such materials.

The right approach to elucidate the phonon confinement effect is to use a 3D dispersion function instead of 1D dispersion curves

$$I(\omega) \cong \iiint_{-\infty}^{\infty} \frac{\exp(-q^2\sigma^2/12)}{(\omega - \omega(q))^2 + (\Gamma_0(\sigma)/2)^2} dq_x dq_y dq_z. \quad (3)$$

The Fourier coefficients in the formula (3) are taken after the work of Roodenko *et al.*:[1] $|C(q_0, q)|^2 = \exp(-q^2\sigma^2/12)$, where it was derived from the comparison with the square confinement function. One more important improvement of the model is to integrate not from 0 to 1, but from $-\infty$ to ∞, which is more correct way since the lattice periodicity is

broken.[1] The difference becomes significant for small crystals, and, since in this work we apply the model to detonation nanodiamond with characteristic size below 4 nm, it becomes important. Note that the lattice constant of diamond is 0.3567 nm.[5] In order to describe real samples, whose size is typically far from being monodisperse, one must take into account the particle size distribution (PSD) $\rho(\sigma)$, which makes the working formula as follows:

$$I(\omega) \cong \int \rho(\sigma) d\sigma \frac{\sigma^3}{N(\sigma)}$$
$$\times \iiint_{-\infty}^{\infty} \frac{\exp(-q^2\sigma^2/12)}{(\omega-\omega(q))^2 + (\Gamma_0(\sigma)/2)^2} dq_x dq_y dq_z,$$

(4)

where $N(\sigma)$ is the normalizing factor:

$$N(\sigma) = \int d\omega \iiint_{-\infty}^{\infty} \frac{\exp(-q^2\sigma^2/12)}{(\omega-\omega(q))^2 + (\Gamma_0(\sigma)/2)^2} dq_x dq_y dq_z.$$

(5)

Although the 3D approach is more complex, it is more consistent and provides a physically meaningful basis for the interpretation of the Raman spectra. We test this model on diamond nanoparticles (ND), which is a good model system for two reasons: (1) diamond gives a distinct band in Raman spectrum; (2) since it is quite well studied, reliable experimental data on the phonon dispersion are available (see below). In addition, with ND becoming increasingly important in nanomedicine and other applications,[6, 7] the estimation of the nanodiamond size is also an important practical task.

The experimental challenge in Raman spectroscopy of nanodiamond is to avoid the laser heating, because the sample is black (5% colloid) or brown (<1%), and hence easily absorbs the laser light. It should be mentioned that such color is typical for detonation ND,[8] probably due to lattice defects (this follows from the fact that extensive surface oxidation does not change the absorbance, although the significant decrease of graphene-like carbon is observed in Raman spectra – data not shown). It has been shown that the heating makes a significant distortion of the Raman spectral pattern of ND.[9] Another problem is to detect the "true" PSD averaged spectrum, rather than a local one (i.e., taken at one point). In previous works on ND,[10–12] the Raman measurements were mostly done for solid (powder) samples under a microscope. That makes the laser heating inevitable, and the PSD is detected at a particular point of the sample. In the present work, in order to make the experimental results more reliable, we measured 5% aqueous colloid[13] of ND in a rotating glass tube (NMR tube). The rotating cell is a standard technique in resonance Raman spectroscopy, used to minimize the effect of the sample degradation by the laser.[14] In our case, the rotation reduces the laser heating of the sample, resulting in almost no thermal distortion of the spectrum. Moreover, it ensures also the averaging of the particle size distribution over the sample. Raman spectra were taken in a back scattering configuration. The 488-nm excitation laser was focused with an objective lens (×40, NA 0.6). The laser power at the sample point was 4.5 mW. Raman intensity was calibrated with a standard tung-
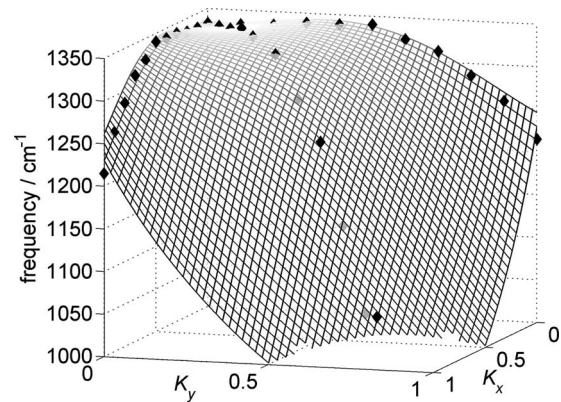

FIG. 1. Phonon dispersion sheet in [100] and [110] directions for the longitudinal optical phonons in the 1st BZ together with the experimental points used for fitting.

sten lamp (LS-1-CAL, Ocean Opt.). The slit function of the measurement was 2.5 cm^{-1} in FWHM.

We studied two different ND samples. One was the detonation nanodiamond (DND) from the Nano Carbon Research Institute (Japan) with the size, estimated by dynamic light scattering (DLS) to be 3.0 ± 0.5 nm. The real PSD for this sample is unknown, because DLS measures hydrodynamic size, which is typically larger that the particle size due to the aggregation and the surface contribution. The second sample was high pressure/high temperature (HPHT) nanodiamond provided by Microdiamant AG (Switzerland) with the particle size of 68 ± 25 nm and the known PSD from the manufacturer.

As was mentioned above, it is very important to use an accurate dispersion function in the case of diamond, because the longitudinal phonon branch shows over-bending. Strictly speaking, the phonon dispersion in diamond, as seen from the work of Warren *et al.*,[15] is a 6-dimensional hyper-surface. However, to be able to work with the phonon confinement model, we have to approximate it with six 3D dispersion functions (3 acoustical and 3 optical). The reliable experimental data on the phonon dispersion are available only along the principal symmetry direction, and to construct analytical form for $\omega(q)$, we have to fit these data with some function. In this work we used 4th degree 3D polynomials, symmetrized according to the symmetry of the Brillouin zone. The data on the phonon dispersion were taken from inelastic neutron scattering[5, 15, 16] and inelastic X-ray scattering[4, 17] experiments (total 220 points). Due to the symmetry, we need accurate description of the phonon dispersion only inside a narrow sector of the first BZ between [100], [111], and [110] directions; for the other points, we simply use rotation and/or translation into this sector. In Fig. 1 is shown the fitted dispersion sheet for the longitudinal optical phonons (which shows the over-bending) in the 1st BZ together with the experimental points. The average rms deviation in all six 3D dispersion function from the experimental points is below 20 cm^{-1}, and is close to 0 near the BZ center. Since the natural Raman bandwidth for small particles (which mainly contribute to the high-q part of the spectrum) is >100 cm^{-1}, the six functions give a good description of the phonon dispersion in ND.

In order to achieve a reasonable speed of integration, Gauss–Hermite quadrature was used with the number of roots of 30 to 90 depending on the particle size (more roots for smaller particles). All fits were performed as a bound constrained optimization in a Matlab script, with the Γ_0 for maximum-contribution domains limited between 4 and 200 cm^{-1} as follows from the overall shape of the Raman pattern. The frequency correction and Boltzmann factor were taken into account while comparing the experimental and calculated spectra.[18]

As of the natural bandwidth (Γ_0 in formula (3)), it was shown in several works that the experimental Γ_0 cannot be simply described by the inverse dependence on the particle size, as one should expect only from the size-dependent phonon lifetime.[19–21] The physical model of this phenomenon is quite complex, hence for the fitting purposes we have chosen the function with three fitting parameters (A, B, n) allowing for certain flexibility (Eq. (6)):

$$\Gamma_0(\sigma) = \Gamma_0(\infty) + \frac{A}{(\sigma - B)^n}. \qquad (6)$$

Since the natural bandwidths in Eqs. (5) and (6) are unknown (to the best of our knowledge, such data for monodisperse samples are absent in the literature), it is necessary to derive Γ_0 from the experiment. To do it in a most reliable way, however, it is highly desirable to know the PSD, because in such case the fit can be made only with 3 parameters (Eq. (6)). Otherwise, one has to derive both PSD and bandwidth from the same fit, which is more difficult.

Therefore, for the HPHT sample, the fit (Fig. 2(a)) was done with a known PSD to derive the Γ_0 parameters for the particles larger than 45 nm (right side of Fig. 3). Next step, having these values as a starting point, the fit was done for the DND, with both Γ_0 and PSD parameters derived from the fit (Fig. 2(b)). Again, the fit reproduces the highly asymmetrical band shape well. It was found from the fit that the PSD has a single maximum at 2.0 nm, and includes particles in the range from 1 to 35 nm (Fig. 3).

In a number of preceding works on nanodiamond[10–12] the fit of the Raman spectra was done assuming monodisperse particles. Our results, however, show that the Raman pattern is very different from that of any hypothetical monodisperse particles (Fig. 4). Importantly, although the amount of the crystallites above 4.6 nm is very small (~0.21% from the fit), the contribution from them is quite significant, because the Raman cross-section scales as a size cube: size-weighted concentration for >4.6 nm particles is ~36% (see Figs. 2(b) and 3, highlighted area). The spectra of monodisperse particles, predicted by the model, well agree with the previous quantum-chemical calculations of Raman spectra of small-size diamonds.[22]

Strictly speaking, the size distribution derived from the Raman spectra reflects the size of a coherently scattering domain rather than the particle size. In case of nanodiamonds we can assume that it is roughly the crystallite size of a diamond core. Hence, one should expect the maximum of Raman PSD to be somewhat smaller than the particle size, because the structure of DND particles is quite complex with 1-2 layers of
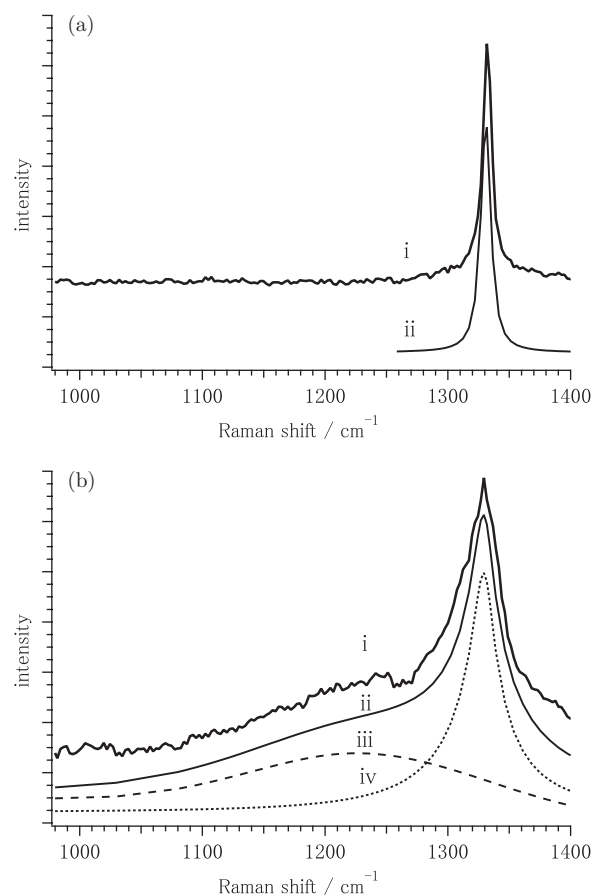

FIG. 2. (a) Experimental Raman spectra for HPHT-nanodiamond (i) and fit with formula (5) (ii). (b) Same for DND. Lines (iii) and (iv) show the contribution from particles smaller and larger 4.6 nm into the total intensity, respectively.

graphene-like carbon on the surface[23] and probably some intermediate sp^{2+x}-carbon in between. Taking this into account, the diamond core should be at least 0.6 nm smaller than the particle size. PSD from DLS (3.0 ± 0.5 nm) measures the hydrodynamic diameter in colloid. Since the particle size should be considerably smaller than the hydrodynamic diameter, the
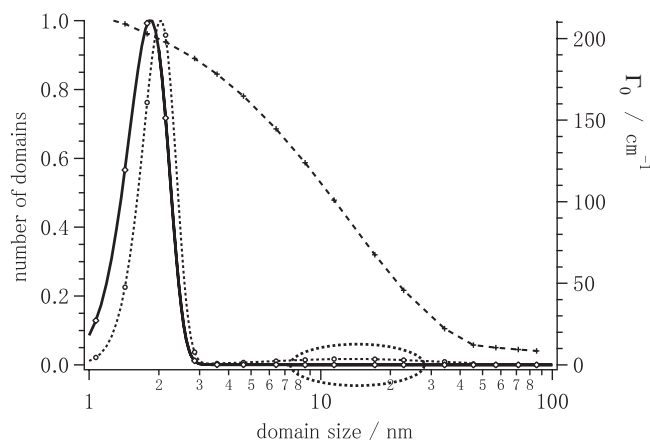

FIG. 3. PSD of DND derived from the Raman spectrum (solid line), the contribution of the particles in Raman spectrum, i.e., size^3-weighted PSD (dotted line), and the natural bandwidth (dashed line).
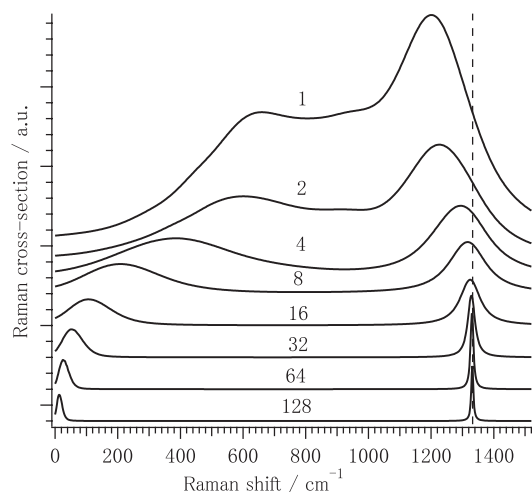
FIG. 4. Hypothetical Raman spectra of single-size diamond particles, normalized and scaled by 1/size. Numbers above the curves indicate size in nm; dashed line is the frequency of the BZ-center phonon (1332.5 cm^{-1}).

maximum of Raman PSD (2.0 nm) is in excellent agreement with the DLS data.

At present, the practical usefulness of the proposed model is limited, because the experimental data on small particles are not very reliable (due to size^3-scaled Raman cross-section the contribution for small particles is relatively low). In the future, it is desirable to measure the spectra of quasi-monodisperse samples as standards to check the reliability of the bandwidth parameters.

Moreover, one should keep in mind that the Raman spectra are sensitive only to the size of the diamond core, while the effective particle size in colloid is a completely independent value.[24,25]

In conclusion, we propose a physically consistent way of interpreting Raman spectra of nanoparticles. Since the 3D dispersion function takes into account the anisotropy of the phonon dispersion, the model built in this way has a straightforward physical meaning. We also show that, in order to provide the correct interpretation of the Raman spectra of small nanoparticles, it is critical to take into account the particle size distribution in an appropriate way.

[1]K. Roodenko, I. Goldthorpe, P. McIntyre, and Y. Chabal, Phys. Rev. B **82**, 115210 (2010).
[2]H. Richter, Z. P. Wang, and L. Ley, Solid State Commun. **39**, 625 (1981).
[3]J. Ager, D. Veirs, and G. Rosenblatt, Phys. Rev. B **43**, 6491 (1991).
[4]J. Kulda, H. Kainzmaier, D. Strauch, B. Dorner, M. Lorenzen, and M. Krisch, Phys. Rev. B **66**, 241202 (2002).
[5]J. Yarnell, J. Warren, and R. Wenzel, Phys. Rev. Lett. **13**, 13 (1964).
[6]E. K. Chow, X.-Q. Zhang, M. Chen, R. Lam, E. Robinson, H. Huang, D. Schaffer, E. Osawa, A. Goga, and D. Ho, Sci. Transl. Med. **3**, 73ra21 (2011).
[7]V. N. Mochalin, O. Shenderova, D. Ho, and Y. Gogotsi, Nat. Nanotechnol. **7**, 11 (2011).
[8]M. Ozawa, M. Inaguma, M. Takahashi, F. Kataoka, A. Krüger, and E. Ōsawa, Adv. Mater. **19**, 1201 (2007).
[9]M. Chaigneau, G. Picardi, H. A. Girard, J.-C. Arnault, and R. Ossikovski, J. Nanopart. Res. **14**, 955 (2012).
[10]M. Yoshikawa, Y. Mori, M. Maegawa, G. Katagiri, H. Ishida, and A. Ishitani, Appl. Phys. Lett. **62**, 3114 (1993).
[11]S. Osswald, V. Mochalin, M. Havel, G. Yushin, and Y. Gogotsi, Phys. Rev. B **80**, 075419 (2009).
[12]A. K. Arora, T. Ravindran, G. L. Reddy, A. K. Sikder, and D. Misra, Diam. Relat. Mater. **10**, 1477 (2001).
[13]A. Krüger, F. Kataoka, M. Ozawa, T. Fujino, Y. Suzuki, A. E. Aleksenskii, A. Y. Vul', and E. Ōsawa, Carbon N. Y. **43**, 1722 (2005).
[14]W. Kiefer and H. J. Bernstein, Appl. Spectrosc. **25**, 500 (1971).
[15]J. Warren, J. Yarnell, G. Dolling, and R. Cowley, Phys. Rev. **158**, 805 (1967).
[16]M. Schwoerer-Böhning, A. Macrander, and D. Arms, Phys. Rev. Lett. **80**, 5572 (1998).
[17]J. Kulda, B. Dorner, B. Roessli, H. Sterner, R. Bauer, T. May, K. Karch, P. Pavone, and D. Strauch, Solid State Commun. **99**, 799 (1996).
[18]R. Shuker, and R. Gammon, Phys. Rev. Lett. **25**, 222 (1970).
[19]S. Kelly, F. H. Pollak, and M. Tomkiewicz, J. Phys. Chem. B **101**, 2730 (1997).
[20]A. Pottier, S. Cassaignon, C. Chanéac, F. Villain, E. Tronc, and J.-P. Jolivet, J. Mater. Chem. **13**, 877 (2003).
[21]M. Salis, P. C. Ricci, and A. Anedda, Open Condens. Matter Phys. J. **2**, 15 (2009).
[22]W. Li, S. Irle, and H. A. Witek, ACS Nano **4**, 4475 (2010).
[23]A. S. Barnard and M. Sternberg, J. Mater. Chem. **17**, 4811 (2007).
[24]M. V. Korobov, D. S. Volkov, N. V. Avramenko, L. A. Belyaeva, P. I. Semenyuk, and M. A. Proskurnin, Nanoscale **5**, 1529 (2013).
[25]O. A. Williams, J. Hees, C. Dieker, W. Jäger, L. Kirste, and C. E. Nebel, ACS Nano **4**, 4824 (2010).